*International Journal of Microwave and Wireless Technologies*, 2009, 1(5), 423–429. 
doi:10.1017/S175907870999064X

# Optically modulated III–V nitride-based high-power IMPact Avalanche Transit Time oscillator at Millimeter-wave window frequency

MOUMITA MUKHERJEE AND SITESH KUMAR ROY

*Extensive simulation experiments are carried out for the first time, to study the optical modulation of the high- frequency characteristics of III–V GaN-(gallium nitride) based top-mounted and flip-chip IMPact Avalanche Transit Time (IMPATT) oscillators at MM-wave window frequency (140.0 GHz). It is found that the un-illuminated GaN IMPATT is capable of delivering a RF power of 5.6 W with an efficiency of 23.5% at 145.0 GHz. Frequency up-chirping of 6.0 GHz and a degradation of RF power output by almost 15.0% are further observed in case of photo-illuminated FC IMPATT. The study reveals that compared to predominate electron photocurrent in top-mounted IMPATT, photo-generated leakage current dominated by hole in flip-chip IMPATT has more pronounced effect on the GaN-based device as regards the frequency chirping and decrease of negative conductance and total negative resistance per unit area of the device. The inequality in the magnitudes of electron and hole ionization rates in the wide band gap semiconductor has been found to be correlated with the above results. The study reveals that GaN IMPATT is a potential candidate for replacing conventional IMPATTs at high-frequency operation. These results are useful for practical realization of optically controlled GaN-based high-power IMPATTs for application in MM-wave communication systems.*

**Keywords:** III–V GaN, Flip-chip diode, Top-mounted diode, IMPATT oscillator, Photo-illumination, Optical modulation, MM-wave window frequency, Carrier ionization coefficient

Received 20 March 2009; Revised 27 July 2009; first published online 19 January 2010

## I. INTRODUCTION

IMPact Avalanche Transit Time (IMPATT) diodes are regarded as the most potential solid-state sources for the generation of RF power in the Millimeter (MM)-wave frequency range, i.e. from 30 to 300 GHz. Low atmospheric attenuation and high penetrating power of MM-wave signals through cloud, dust, and fog at atmospheric window frequencies have made millimeter-wave communication systems very attractive. The 140.0 GHz frequency (D-band) is very important atmospheric window frequency around which research activities in the field of MM-wave communication and RADAR systems are centered. In recent years, researchers have focused their attention on the development of high-power IMPATT devices in the MM-wave window frequencies. Conventional Si-, GaAs-, and InP-based IMPATTs are found to the reliable but these are limited by power and operating frequencies. Due to its high breakdown electric field ($E_C$: $3.0 \times 10^6$ V/m), wide band-gap ($E_g$: 3.45 eV), high carrier saturation velocity ($v_S$: $3.05 \times 10^7$ m/s), and high thermal conductivity (K: 2.25 W/cm/K), gallium nitride (GaN) has been recognized as the most promising candidate for high-power semiconductor devices [1]. These material parameters of GaN are very much conducive for generating high RF power from IMPATT devices based on this material, as the RF power output from an IMPATT is proportional to $E_C^2 v_S^2$. Recently, high-quality GaN epilayers are grown on Si (111) substrate by MOCVD by using a $Si_xN_y$ inserting layer [2]. These $Si_xN_y$ inserting layers can efficiently counteract the propagation of misfit dislocation usually observed in GaN epilayers grown on Si substrates and also improve the crystalline quality [2]. This has helped GaN to emerge as relatively mature wide-band-gap semiconductor for developing high-frequency devices. Thus in the light of maturity of the fabrication technology and the unique material parameters, GaN appears to be the best choice, overall, for the next decade of device development at MM-wave region.

Ever since the emergence of IMPATT oscillators as high-power source, the possibilities of controlling the high-frequency properties using external agencies like optical radiation has received considerable attention of device engineers, owing to its practical application in optoelectronic integrated circuits, millimeter-wave integrated circuits, and phased array antennas for space-based communication and imaging. Previous experimental studies on photo-illuminated conventional (Si- and GaAs-based) IMPATTs showed that the photo-generated carriers reduce the output power and efficiency of the device along with an increase of its tuning range in the MM-wave band [3, 4]. The composition of leakage current as regards the hole (in flip-chip illumination configuration) and electron (in top-mounted illumination configuration) components plays an important role in the optical control of IMPATT diodes. Vyas *et al.* [3] demonstrated that the

Centre of Millimeter-Wave Semiconductor Devices and Systems (Cmsds, A Joint Venture Between Drdo, Ministry Of Defence, Govt. of India and University of Calcutta), Centre of Advanced Study in Radiophysics and Electronics, University of Calcutta 1, Girish Vidyaratna Lane, Kolkata 700009, West Bengal, India.
**Corresponding author:**
M. Mukherjee
Emails: mou_mita_m@yahoo.com, mukherjee_mita@hotmail.com

output power and efficiency of an Si X-band IMPATT oscillator vary more appreciably with electron-dominated photo-current than the hole-dominated photo-current. Further, recent simulation experiment has shown that in case of WBG SiC and InP-based illuminated IMPATTs, the situation is just reversed [5–8], i.e. the hole-dominated photo-current is more pronounced in modulating the high-frequency characteristics of the devices in MM-wave region. Thus, these interesting results have prompted the authors to study the relative roles of electron- and hole-dominated photo-generated leakage current in modulating the high-frequency admittance and negative resistivity characteristics of the TM and FC GaN IMPATT devices.

## II. COMPUTER SIMULATION METHODOLOGIES

In the simulation scheme, one-dimensional p–n junction diode equations (Poisson and current continuity equations), considering the mobile space charge effect, have been solved by a double iterative computer method [9], satisfying appropriate boundary conditions as described earlier [5–8]. Two types of SDR IMPATT structures are mostly fabricated: $n^{++}$ p $p^{++}$ and $p^{++}$ n $n^{++}$. However, the later is considered to be better because technology of $n^{++}$ substrate is more advanced and better understood than $p^{++}$ substrate. Further, the extent of the un-depleted region between the edge of the depletion region and interface of epitaxy and substrate (un-swept epitaxy) which contributes positive resistance and thereby causes serious power loss is expected to be smaller in GaN-based $p^{++}$ n $n^{++}$ diode, because of higher mobility of electrons than that of holes in GaN [10]. Moreover, for any semiconductor, the avalanche zone width is smallest when the structure is chosen so that the carrier with highest ionization rate drifts towards the junction [11]. It was observed that avalanche zone of $n^{++}$ p $p^{++}$ structure is narrower than its complimentary structure in Si IMPATTs [11] which leads the higher efficiency in $n^{++}$ p $p^{++}$ Si IMPATTs. While the situation is just reversed in InP- and GaAs-based SDR IMPATTs [12, 13]. This is due to the higher ionization rate of electron ($\alpha_n$) than that of the hole ($\alpha_P$) in Si, and on the other hand, lower values of $\alpha_n$ than $\alpha_P$ in GaAs and InP materials [10]. In case of Wz-GaN electron mobility is found to be higher than hole mobility as well as $\alpha_P > \alpha_n$ [10]. The material parameters of Wz-GaN prompted the authors to chose $p^{++}$ n $n^{++}$ structure for modeling high-power, high-efficiency IMPATT devices. In the present analysis, a flat profile SDR ($p^{++}$ n $n^{++}$) structure is thus considered, where, $n^{++}$ and $p^{++}$ are highly doped substrates and cap layers, respectively, and n is the epilayer.

During its operation at MM-wave region, IMPATT diode generates a substantial amount of heat, which results in an increase of the diode junction temperature that plays a significant role on the performance of the IMPATT diode. The authors have, therefore, considered the Monte Carlo simulated values of saturated drift velocity and mobility of charge carrier in GaN within the range 300 K $< T <$ 600 K [10, 14] for the present analysis. Experimental ionization rate data of charge carrier [15] have been extrapolated to the high-temperature (mentioned earlier) ionization rate data, and are incorporated in the simulation. Realistic exponential function and complimentary error function at the junction as well as at $n^{++}$ n contact region have been incorporated in the analysis [5]. The diode structure has been designed, considering n region width approximately by the simple transit time equation [16]

$$W_n = 0.37\, v_{ns}/f_o, \tag{1}$$

where $v_{ns}$ is the electron saturated velocity and $f_o$ is the design frequency. The tunneling effect has been ignored because of the wide band gap of GaN and relatively moderate doping in the active region. The space step for the present simulation technique is taken as $\sim 10^{-9}$ m.

The static characteristics, such as, electric field profile and normalized current density profile of the designed diode are obtained following the method described elsewhere [5–8]. With the static output parameters as input, the spatial variation of diode negative resistivity ($R$) and the reactivity ($X$) in the depletion layer have been obtained solving two second-order differential equation in $R$ and $X$, described elsewhere [5–8]. A double iterative simulation technique is adopted for solving the two equations [9]. The total integrated negative resistance ($Z_R$) and reactance ($Z_X$) of the diodes at a particular frequency $\omega$ can be determined from the numerical integration of the resistivity ($R$) and the reactivity ($X$) profiles over the depletion layer, as described in earlier articles [5–8]. The diode negative conductance (G) and susceptance ($B$) are calculated from the following expressions:

$$\begin{aligned} G(\omega) &= -Z_R/[(Z_R)^2 + (Z_X)^2] \quad \text{and} \\ B(\omega) &= Z_X/[(Z_R)^2 + (Z_X)^2]. \end{aligned} \tag{2}$$

$G$ and $B$ are functions of frequency and RF voltage ($V_{RF}$).

The conversion efficiency ($\eta$) is calculated from the approximate formula [17]

$$\eta(\%) = (V_D \times 100)/(\pi \times V_B), \tag{3}$$

where $V_D$ is the normalized voltage drop, i.e. $V_D = V_B - V_A$ with $V_A$ being the voltage drop across the avalanche region, and $V_B$ the breakdown voltage. The validity of using equation (3) for determining $\eta$ as well as the validity of the computer methodology was previously verified for InP [18]- and Si [19]-based IMPATTs. Based on the above-mentioned computer methodology, breakdown voltage and efficiency were computed for an X-band InP IMPATT diode and are found to be 57.7 V and 11.7% against the corresponding experimental values of 60 V and 11.1%, respectively [18]. Later, 60 GHz Si IMPATT diode was fabricated [19] based on the design data as obtained by the DC analysis, discussed elsewhere. A general agreement of simulated and experimentally observed results is found [19]. In spite of this general agreement of those experimental results with the simulations, it should be mentioned that a more accurate computation of device efficiency requires full simulation of the IMPATT diode embedded in a suitable MM-wave cavity which considers the device–circuit interaction. However, the intrinsic performance of a given device can be estimated using the Scharfetter–Gummel formula (equation (3)) by accurately evaluating the field profile in the depletion layer.

A small-signal-based power ($P_{RF}$) evolution is carried out from the following equation [20]:

$$P_{RF} = (V_B/2)^2 \times G_P \times A/2, \tag{4}$$

https://doi.org/10.1017/S175907870999064X Published online by Cambridge University Press

where $G_P$ is the device negative conductance at peak frequency and the device area ($A$) is considered as 100 μm². However, a more precise estimate of the power capability of the SDR device requires full consideration of voltage swing, thermal limitations, and the device–circuit interaction.

The avalanche frequency ($f_a$) is the frequency at which the imaginary part ($B$) of the admittance, i.e. device susceptance, changes its nature from inductive to capacitive. Again it is the minimum frequency at which the real part ($G$) of admittance becomes negative. At the avalanche frequency, oscillation starts to build up in the circuit. For an ideal read diode, according to Gilden and Hines [21], $f_a$ is given by

$$f_a = (1/2\pi)(2\alpha' v_s J_o/\varepsilon_o \varepsilon_r)^{0.5}, \quad (5)$$

where $J_o$ is the bias current density, $\alpha' = d\alpha/dE$, $\alpha = \alpha_n = \alpha_P$, and $v_S = v_{ns} = v_{ps}$. However, the computer program adopted in the present analysis [5, 6, 9], for modeling and analyzing the small-signal behavior of high-frequency IMPATT devices, is free from such simplifying assumptions as done by Gilden and Hines [21]. In the present generalized simulation technique [9], $\alpha_n \neq \alpha_P$, $v_{ns} \neq v_{ps}$, and the value of $f_a$ at any $J_o$ is obtained from the admittance plot of the diode corresponds to the frequency at which $B$ changes its sign from negative to positive.

The leakage current entering the depletion region of the reversed biased p–n junction of an un-illuminated IMPATT diode is only due to thermally generated electron–hole pairs and it is so small that the multiplication factors ($M_{n,p}$) become very high:

$$M_n = J_o/(J_{ns})_{th} \quad \text{and} \quad M_p = J_o/(J_{ps})_{th} \quad (6)$$

where $J_o$ is the bias current density, and $(J_{ns})_{th}$ and $(J_{ps})_{th}$ are the leakage current densities due to thermally generated electrons and holes, respectively.

When optical radiation of suitable wavelength (photon energy, $hc/\lambda > E_g$) is incident on the active layer of the device, the leakage current increases significantly due to photo-generation of charge carriers. The leakage current is multiplied by impact ionization in the high field region of the diode. The current multiplication factors under optical illumination are given by

$$M_n = J_o/[J_{ns(th)} + J_{ns(opt)}] \quad \text{and} \quad M_p = J_o/[J_{ps(th)} + J_{ps(opt)}], \quad (7)$$

where $J_{ns\ (opt)}$ and $J_{ps\ (opt)}$ are the leakage current densities due to optically generated electrons and holes, respectively, which depend on the incident optical power according to the following equation [13]:

$$(J_{ns} \text{ or } J_{ps})_{opt} = q\eta P_{opt}/Ah\nu, \quad (8)$$

where $\eta$ is the quantum efficiency and $A$ is the surface area over which absorption of incident optical power $P_{opt}$ takes place corresponding to photon energy $h\nu$ ($\nu$ is the frequency of incident radiation). If recombination is neglected, a linear response of the avalanche breakdown can be assumed, and $(J_{ns})_{opt}$ or $(J_{ps})_{opt}$ would increase linearly with $P_{opt}$ over a particular range of wavelengths in which appreciable absorption takes place. From equation (7) it is clear that the enhancement of the leakage current under optical illumination of the devices is manifested as the lowering of $M_{n,p}$. The validity of the simulation scheme was reported earlier [5–8].

The effect of shining light from the junction side ($p^{++}$ side, Fig. 1(a)) in a TM $p^{++}$ n $n^{++}$ IMPATT structure is to generate an electron-dominated photo-current and thereby reduces $M_n$ to much smaller values, leaving $M_p$ at its large value ($\sim 10^6$). Similarly the effects of shining light from the substrate side ($n^{++}$ edge, Fig. 1(b)) in an FC $p^{++}$ n $n^{++}$ IMPATT structure is to generate a hole-dominated photo-current and thereby reduces $M_p$ to much smaller values, leaving the electron multiplication factor $M_n$ practically unchanged at its large value ($\sim 10^6$). In order to assess the role of leakage currents in controlling the dynamic properties of IMPATT oscillator at THz frequency, simulation experiments are carried out on the effect of $M_n$ (keeping $M_p$ very high $\sim 10^6$) and $M_p$ (keeping $M_n$ very high $\sim 10^6$) on (i) the small-signal admittance characteristics, (ii) the negative resistivity profiles, (iii) quality factor at peak frequencies ($Q_p$), and (iv) the RF power output of SDR GaN IMPATT.

## III. RESULTS AND DISCUSSIONS

Simulation experiments predict that the designed GaN-based diode may generate output power of 5.6 W with an efficiency of 23.5%. The DC and small-signal output data are shown in Table 1. The authors have further compared the performances of the Wz-GaN-based IMPATTs with those of conventional Si-, GaAs- and InP-based D-band IMPATT diodes under almost similar operating conditions. Electric field profiles of the designed diodes are shown in Fig. 2. The DC and small-signal results of the diodes are shown in Table 1. It is found that peak electric field, breakdown voltage, and efficiency are much higher in case of GaN IMPATT at $J_o = 4\times10^8$ A/m². The much higher values of breakdown voltage and efficiency in GaN IMPATT are due to its high carrier saturation velocity compared to other semiconductors. It is also very interesting to observe that in case of GaN IMPATT, output power improves significantly (Table 1). Thus, the comparative study definitely establishes the potential of GaN IMPATT for replacing traditional IMPATTs at D-band operation.

In $p^{++}$ n $n^{++}$ structure, the generated electrons in the avalanche region drift through the n-epilayer towards the $n^{++}$ side. In order to estimate $f_a$ from equation (5), the authors

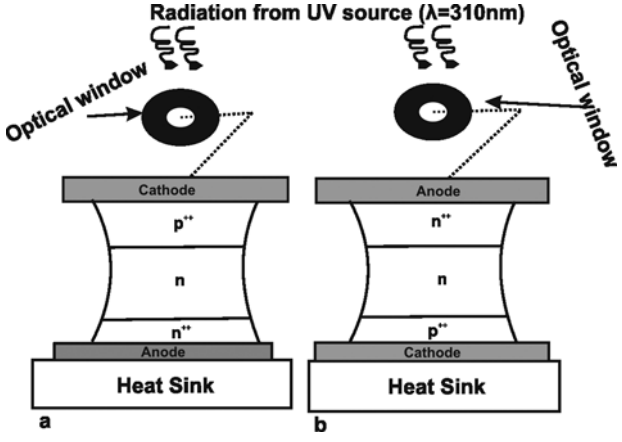


**Fig. 1.** Schematic diagram of (a) top-mounted and (b) flip-chip MM-wave GaN-based SDR IMPATT diode under optical illumination.

https://doi.org/10.1017/S175907870999064X Published online by Cambridge University Press

**Table 1.** DC and MM-wave characteristics of SDR IMPATTs at D-band ($J_o = 4.0\times10^8$ A/m$^2$, doping conc. $= 8.0\times10^{22}$ m$^{-3}$).

| SDR diode parameters | Si | GaAs | InP | Wz-GaN |
|---|---|---|---|---|
| Peak electric field ($E_m$) ($10^8$ V/m) | 0.65 | 0.53 | 0.70 | 3.25 |
| Breakdown voltage ($V_B$) (V) | 8.3 | 11.0 | 10.5 | 102.0 |
| Efficiency ($\eta$) (%) | 6.0 | 8.2 | 15.0 | 23.50 |
| Peak operating frequency ($f_p$) (GHz) | 143 | 140.0 | 146.0 | 145.0 |
| Peak negative conductance ($-G_p$) ($10^6$ S/m$^2$) | 27.0 | 31.0 | 45.0 | 43.0 |
| Device quality factor ($-Q_p$) | 2.7 | 2.3 | 2.4 | 1.90 |
| RF power output ($P_{RF}$) (W) | 0.023 | 0.047 | 0.062 | 5.6 |
| Negative resistance at peak ($-Z_{RP}$) ($10^{-9}$ $\Omega$ m$^2$) | 4.4 | 5.1 | 3.2 | 5.04 |

have taken $J_o = 4 \times 10^8$ A/m$^2$, $\alpha = \alpha_n$, $v_S = v_{ns}$, and $d\alpha/dE$ is simulated from $\alpha(E)$ characteristics. The resonant avalanche frequency of GaN-based un-illuminated IMPATT, as calculated from equation (5), is 42.5 GHz. However, the adopted generalized simulation technique [9] predicts a little higher value of $f_a$ ($f_a = 48$ GHz). The discrepancy in the values of $f_a$ is due to the difference in the modeling techniques developed by Gilden and Hines [21] and Roy *et al.* [9], as discussed in Section II. Figure 3 shows the variation of ionization rate with active region width in case of GaN diode. It is found that $\alpha_n$ decrease rapidly away from the junction and the value becomes significantly low at around 27% of the total epilayer width. Thus within 27% of the total layer width of GaN SDR, a large number of e–h pair are generated by impact ionization.

Device negative resistance ($-Z_R$) and reactance ($-Z_X$) are simulated through the adopted computer simulation technique [5–9]. The plot of variation of impedance of the GaN IMPATT with frequency is shown in Fig. 4. The graphs show that the devices posses negative resistance for all frequencies above the avalanche frequency ($f_a$), where its reactance is capacitive. This is due to the fact that, in the oscillating frequency range, the magnitude of $Z_R$ is found to be small compared to $Z_X$. This is also evident from Fig. 4 that the values of $|-Z_R|$ and $|-Z_X|$ decrease as the operating

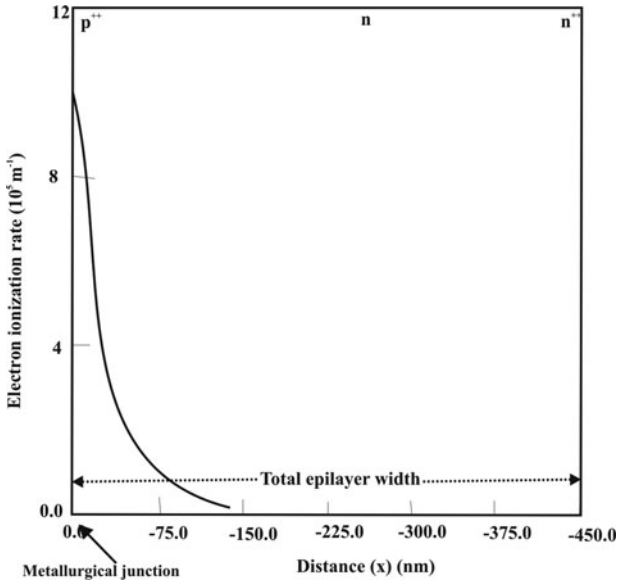


**Fig. 3.** Electron ionization rate versus distance in the space-charge layer of a SDR GaN D-band IMPATT diode.

frequency increases. The above results are in trend agreement with the basic IMPATT characteristics [16].

The effects of electron- and hole-dominated photocurrents on the MM-wave performance of the GaN IMPATT is presented in Table 2. The admittance characteristics of the un-illuminated and illuminated TM and FC diodes are plotted in Figs 5(a) and 5(b), respectively. The figures show that the values of $|-G_P|$ of the diode decrease with the lowering of $M_n$ and $M_P$. At the same time, the frequency range over which the device exhibits negative conductance shifts towards higher frequencies with the lowering of $M_n$ or $M_P$. The output

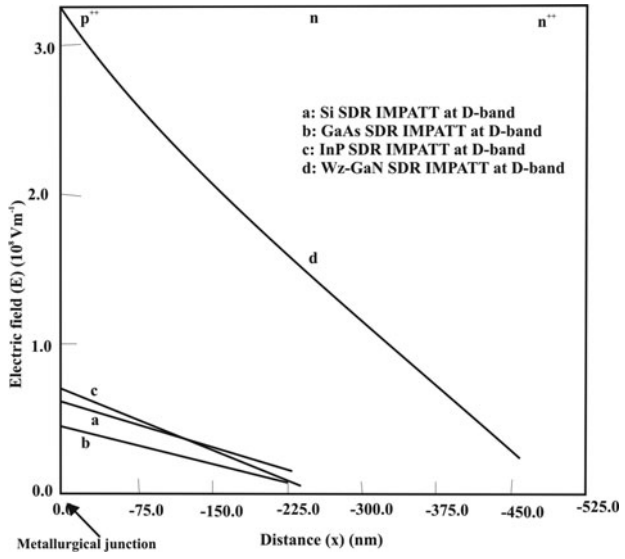


**Fig. 2.** Electric field profiles of Si, GaAs, InP, and GaN IMPATTs at D-band.

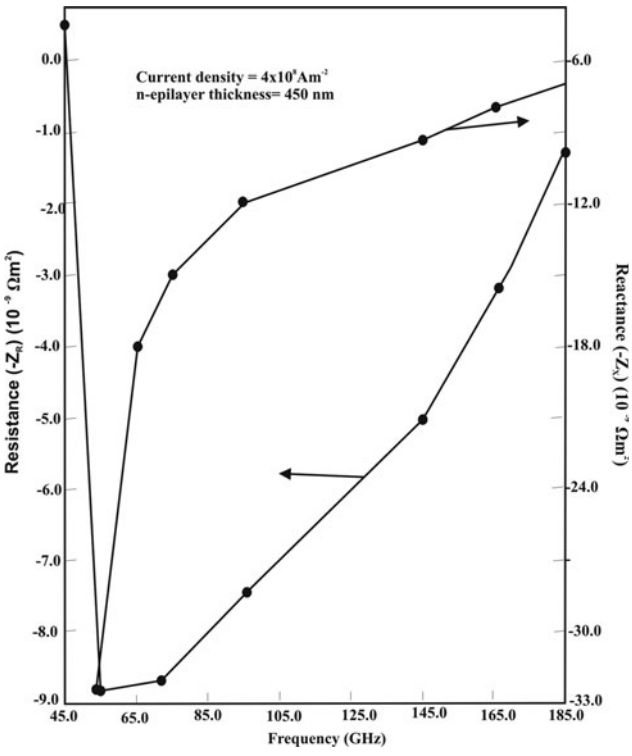


**Fig. 4.** Impedance plot of Wz-GaN-based SDR IMPATT at D-band.

https://doi.org/10.1017/S175907870999064X Published online by Cambridge University Press

**Table 2.** Output data of optically modulated GaN-based SDR IMPATT at 140.0 GHz window.

| Diode type | $M_n$ | $M_P$ | $-G_P$ ($10^6$ S/m$^2$) | $-Z_{RP}$ ($10^{-9}$ Ω m$^2$) | $f_P$ (GHz) | $Q_P$ | $P_{RF}$ (W) |
|---|---|---|---|---|---|---|---|
| Un-illuminated | $10^6$ | $10^6$ | 43.0 | 5.0 | 145.0 | 1.9 | 5.6 |
| TM | 50 | $10^6$ | 41.2 | 4.36 | 147.0 | 2.13 | 5.36 |
| TM | 25 | $10^6$ | 38.5 | 3.87 | 149.0 | 2.38 | 5.00 |
| FC | $10^6$ | 50 | 40.0 | 4.12 | 149.0 | 2.25 | 5.20 |
| FC | $10^6$ | 25 | 36.7 | 3.67 | 151.0 | 2.53 | 4.77 |

data for illuminated SDR IMPATT (Table 2) indicate that the value of negative conductance at peak frequency $|-G_P|$ decreases by 10.4% when $M_n$ reduces from $10^6$ to 25, corresponding to TM illumination configuration. On the other hand, in case of FC IMPATT diode, lowering of $M_P$ from $10^6$ to 25 causes more (14.6%) reduction in the value of $|-G_P|$. It is worthwhile to mention that the frequency chirping is much prominent (6.0 GHz) in case of FC diode than that in case of TM diode (4.0 GHz) for a similar variation of $M_p$ and $M_n$, respectively. The above results indicate that the hole-dominated photo-current (in FC diodes) has more pronounced effect in modulating the device admittance characteristics than that of electron-dominated photo-current (in TM diode) in GaN-based MM-wave IMPATT devices.

Figures 6(a) and 6(b) show the profiles of negative resistivity at the peak frequencies corresponding to different values of $M_n$ ($M_p = 10^6$) and $M_P$ ($M_n = 10^6$) for flat profile TM and FC diodes, respectively. Negative resistivity profiles give a physical insight into the region of the depletion layer that contributes to RF power. These figures show that in both the illumination configurations, the profiles exhibit negative resistivity peaks in the middle of the drift layer with dips in the avalanche layer close to the junction. Due to the enhancement of electron photocurrent, the negative resistivity peaks are lowered accompanied by a gradual shift in their locations from the middle of the drift layer towards the $n^{++}$ edge. It is also found that the decrease of negative resistivity peaks is more pronounced in illuminated FC diode.

The variation of negative resistance ($Z_{RP}$) and quality factors ($Q_P$) at peak frequencies, with $M_n$ or $M_p$ for TM and FC diodes are shown in Table 2. The oscillator power output depends on the negative resistance but the high-frequency performance of the oscillator under illumination depends on the $Q$-factor. A smaller value of $Q_P$ indicates higher DC to RF conversion efficiency and better stability of oscillation. It is observed from the present studies that the MM-wave power output delivered to the load and conversion efficiency decrease with a shift of operating frequency when the active area of the device is illuminated. It is evident from Table 2 that the magnitude of $Q_P$ is lowest for the un-illuminated diode. It is also depicted from Table 2 that as $M_n$ or $M_P$ decreases from the high value of $10^6$, the magnitude of $Q$-factor increases while $Z_{RP}$ decrease. However, the increase of the $Q$-factor and decrease of the $Z_{RP}$ are sharper for FC illumination configuration than for TM illumination configuration. The results further indicate that a lowering of $M_n$ from $10^6$ to 25 causes a decrease of $Z_{RP}$ by 23% and an increase of $Q_P$ by 25.26%. However for the similar variation of $M_P$, the value of $Z_{RP}$ decreases by 27% and the magnitude of $Q_P$ increases by 33.0%.

The pronounced effect of hole-dominated leakage current in modulating the MM-wave characteristics of the GaN-based IMPATT diode can be interpreted on the basis of the relative magnitudes of hole and electron ionization rates in Wz-GaN for different electric field ranges. The effects of predominate hole and electron photo-currents in FC and TM diodes on the negative resistance profiles and the admittance characteristics can be explained from the ionization integral

$$\int_0^{x_a} (\alpha_p - \alpha_n) dx$$

where $\alpha_P$ and $\alpha_n$ are the hole and electron ionization rates and $x_a$ is the avalanche zone width.

As the magnitude of $\alpha_P > \alpha_n$ for the electric field in the avalanche zone of the Wz-GaN IMPATT [22], the value of the integral will be larger for hole-dominated photo-current corresponding to FC diode structure than for electron-dominated photo-current, corresponding to TM diode structure. This

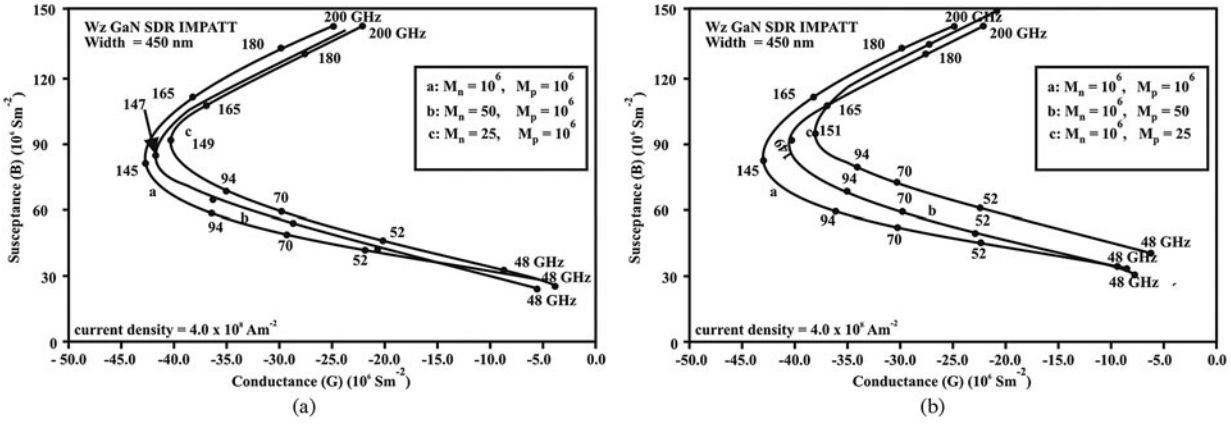


**Fig. 5.** (a) Conductance ($G$) – susceptance ($B$) plots of un-illuminated GaN SDR IMPATT diode (a) and the illuminated diode (b, c) for different values of $M_n$. (b) Conductance ($G$) – susceptance ($B$) plots of un-illuminated GaN SDR IMPATT diode (a) and the illuminated diode (b, c) for different values of $M_p$.

https://doi.org/10.1017/S175907870999064X Published online by Cambridge University Press

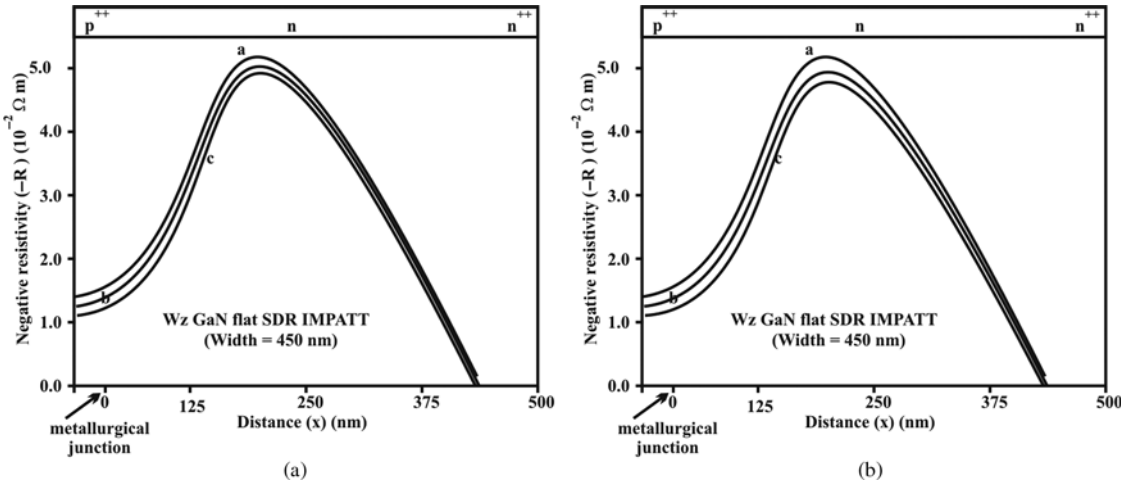


**Fig. 6.** (a) Negative resistivity profiles of the un-illuminated GaN flat profile SDR IMPATT diode (a) and the illuminated diode (b, c) for different values of $M_n$ and corresponding different values of optimum frequencies, $f_p$ in GHz: (a) $M_n = 10^6$, $M_p = 10^6$, $f_p = 145$ GHz; (b) $M_n = 50$, $M_p = 10^6$, $f_p = 147$ GHz; (c) $M_n = 25$, $M_p = 10^6$, $f_p = 149$ GHz. (b) Negative resistivity profiles of the un-illuminated GaN flat profile SDR IMPATT diode (a) and the illuminated diode (b, c) for different values of $M_p$ and corresponding different values of optimum frequencies, $f_p$ in GHz: (a) $M_n = 10^6$, $M_p = 10^6$, $f_p = 145$ GHz; (b) $M_n = 10^6$, $M_p = 50$, $f_p = 149$ GHz; (c) $M_n = 10^6$, $M_p = 25$, $f_p = 151$ GHz.

explains why the MM-wave characteristics of illuminated GaN IMPATT diode is more sensitive to photo-generated hole leakage current in FC illumination configuration. On the other hand, in case of illuminated Si IMPATT, electron-dominated photo-current (in TM structure) is found to play the dominant role in modulating the RF characteristics [3]. This is because the electron ionization rate is greater than the hole ionization rate in Si. Although GaN and Si IMPATTs show opposite behavior with respect to electron- and hole-dominated photo-currents, the nature of optical modulation is similar in both the diodes, as far as the decrease of RF power, increase of optimum frequency, and decrease in the magnitude of negative conductance are concerned.

## IV. CONCLUSIONS

A detailed analysis of the modulation of the MM-wave characteristics of the GaN-based optically illuminated FC and TM IMPATT diodes are reported for the first time at D-band (at around 140.0 GHz window). This study reveals that the predominate hole photo-current has more pronounced effects on GaN-based IMPATTs as regards the frequency up-chirping and decrease of total negative resistance of the diode. The above analyses, if carried out through a large-signal model may provide better quantitative results but, it will not show any qualitative difference from the results obtained from the present small-signal analysis. Since there are no available experimental results on optically illuminated GaN IMPATT, no comparison could be made. The present simulation results may further be used for experimental realization of optically controlled high-power IMPATT oscillator for application in MM-wave communication systems.

## ACKNOWLEDGEMENTS

The authors wish to acknowledge Defence Research and Development Organization (DRDO, Ministry of Defence) Govt. of India, and University Grant Commission, Govt. of India, for their support to carry out this work. Moumita Mukherjee is grateful to DRDO for awarding her Senior Research Fellowship (SRF) to do this work.

## REFERENCES

[1] Buniatyan, V.V.; Aroutiounian, V.M.: Wide gap semiconductor microwave devices. J. Phys. D: Appl. Phys., **40** (2007), 6355–6385.

[2] Lee, K.J.; Shin, E.H.; Kim, J.Y.; Oh, T.S.; Lim, K.Y.: Growth of high quality GaN epilayers with $Si_x$ $N_y$ inserting layer on Si (111) substrate. J. Korean Phys. Soc., **45** (2004), S756–S759.

[3] Vyas, H.P.; Gutmann, R.J.; Borrego, J.M.: The effect of hole versus electron photocurrent on microwave-optical interaction in IMPATT oscillators. IEEE Trans. Electron Devices, **ED-26** (1979), 232–234.

[4] Seeds, A.J.; Forest, J.R.: Optical control of microwave semiconductor device. IEEE Trans. Microwave Theory Tech., **38** (1990), 577.

[5] Mukherjee, M.; Mazumder, N.; Dasgupta, A.: Simulation experiment on optical modulation of 4H-SiC millimeter-wave high power IMPATT oscillator. J. Eur. Microwave Assoc., **4** (2008), 276–282.

[6] Mukherjee, M.; Mazumder, N.; Roy, S.K.: Prospects of 4H-SiC double drift region IMPATT device as a photo-sensitive high power source at THz regime. Active Passive Electron. Compon., **2008** (2008), 1–9. doi:10.1155/2008/275357.

[7] Mukherjee, M.; Mazumder, N.: Optically illuminated 4H-SiC THz IMPATT device. Egypt. J. Solids, **30** (2007), 85–102.

[8] Mukherjee, M.; Mazumder, N.: Comparison of photo-sensitivity of Si and InP IMPATT diodes at 220 GHz, in *Proc. IEEE Int. Conf. on Microelectronics, Electronics and Electronic Technologies MEET 2007*, University of Zagreb, Croatia, 2007, 72–77.

[9] Roy, S.K.; Banerjee, J.P.; Pati, S.P.: A Computer analysis of the distribution of high frequency negative resistance in the depletion layer of IMPATT Diodes, in *Proc. 4th Conf. on Numerical Analysis of Semiconductor Devices (NASECODE IV) (Dublin)* (Dublin: Boole), 1985, 494–500.

[10] Electronic Archive: New Semiconductor Materials, Characteristics and Properties (Online) www.ioffe.ru/SVA/NSM/Semicond.

https://doi.org/10.1017/S175907870999064X Published online by Cambridge University Press

[11] Udelson, B.J.; Ward, A.L.: Computer comparison of $n^+$ p $p^+$ and $p^+$ n $n^+$ junction silicon diodes for IMPATT oscillators. Electron. Lett., **7** (1971), 723.

[12] Banerjee, J.P.; Pati, S.P.; Roy, S.K.: Computer studies on the space charge dependence of avalanche zone width and conversion efficiency of single drift $p^+$ n $n^+$ and $n^+$ p $p^+$ InP IMPATTs. Appl. Phys. A, **35** (1984), 125–129.

[13] Banerjee, J.P.: Some studies on the DC and high-frequency properties of InP and GaAs IMPATT devices, |tPh.D. thesis, University of Calcutta, India, 1984.

[14] Albrecht, J.D.; Wang, R.P.; Ruden, R.P.; Farahmand, M.; Brennan, K.F.: Electron transport characteristics of GaN for high temperature device modeling. J. Appl. Phys., **83** (1998), 4777–4781.

[15] Kunihiro, K.; Kasahara, K.; Takahashi, Y.; Ohno, Y.: Experimental evaluation of impact ionization coefficients in GaN. IEEE Electron Device Lett., **20** (1999), 608–610.

[16] Sze, S.M.: Physics of Semiconductor Devices, 2nd ed., Wiley Publishing, New Delhi, 1982.

[17] Scharfetter, D.L.; Gummel, H.K.: Large signal analysis of a silicon read diode oscillator. IEEE Trans. Electron Devices, **16** (1969), 64–77.

[18] Banerjee, J.P.; Pati, S.P.; Roy, S.K.: A study of indium phosphide single drift and double drift avalanche diodes from computer analysis of field and current profiles. Ind. J. Pure Appl. Phys., **21** (1983), 661–664.

[19] Banerjee, J.P.; Luy, J.F.; Schaffler, F.: Comparison of theoretical and experimental 60 GHz silicon IMPATT diode performances. Electron. Lett., **27** (1991), 1049–1050.

[20] Eisele, H.; Haddad, G.I.: Microwave Semiconductor Device Physics (Ed. S.M. Sze), Wiley, New York, 1997, 343.

[21] Gilden, M.; Hines, M.E.: Electronic tuning effects in read microwave avalanche diode. IEEE Trans. Electron Devices, **ED-13** (1966), 169.

[22] Pearton, S.J.: GaN and Related Materials II, CRC Press, The Netherland, 2000, 340–343.

**Moumita Mukherjee** was born in Kolkata, West Bengal, India, on 13 October 1977. The author has received an M.Sc. degree in physics with specialization in electronics and communication from the University of Calcutta, India, in 2002.

During June 2003–June 2007, she worked as a Senior Research Fellow (SRF) of Defence Research and Development Organization (DRDO), New Delhi, India, at International Institute of Information Technology (IIIT), Visva Bharati University, and Advanced Technology Centre, Jadavpur University, Kolkata, India. She is presently a Ph.D. student in the Department of Radio Physics and Electronics, University of Calcutta. At present, she is attached with Centre of Millimeterwave Semiconductor Devices & Systems (joint venture between DRDO and University of Calcutta), University of Calcutta, as a Senior Research Fellow. Her research interest is focused on the design and fabrication of millimeter and sub-millimeter (terahertz) wave high-power devices based on wide-band-gap semiconductors, study of photo-irradiation effects on the high-power terahertz IMPATT oscillators, optical injection locking of the fabricated devices and nano-scale transit time devices.

She has published more than 30 research papers on transit time devices in several refereed international journals and IEEE-Proceedings.

**Sitesh Kumar Roy** (SM IEEE 2005) was born in Kolkata on 30 April 1937. The author has obtained an M.Sc. (Tech) in radio physics and electronics from University of Calcutta, West Bengal, India. He has received a Ph.D. (Sc) degree in the year 1968, from the University of Calcutta, West Bengal, India. The author's major field of study is microwave and millimeter-wave semiconductor device and systems.

He is a Professor of Radio Physics and Electronics, University of Calcutta, since 1979. He was formerly Head of the Department and Coordinator of Centre of Advanced study in Radio Physics and Electronics, University of Calcutta. He is presently the Director of Centre of Millimeter wave Semiconductor Devices and Systems, University of Calcutta. He has pioneered research activities in microwave and mm-wave IMPATT devices in India, both theoretical and experimental. He has successfully developed indigenous microwave and millimeter-wave Si IMPATT diodes in University of Calcutta. He has presented fast and accurate methods of computer analysis in NASACODE Conferences I and IV, in 1979 and 1985 in Trinity College, Ireland. He has obtained two patents from Govt. of India, on IMPATT oscillators and IMPATT amplifiers. He has published more than 250 research papers in several reputed international journals and conference proceedings. He has supervised more than 14 Ph.D. thesis in the field of semiconductor devices. He is the author of the book "Microwave semiconductor devices" (New Delhi, India: Prentice–Hall of India Private Limited, 2004). He has written another book chapter on "Transit time devices" in Encyclopedia on electrical and electronic engineering by John Wiley and Sons, New York, 1999. His current research interests include experimental and theoretical investigation of millimeter-wave and terahertz devices and systems.

Prof. Roy is the Senior Member of IEEE (USA), Fellow of the Institution of Electronics & Telecommunication Engineers (IETE), India.

https://doi.org/10.1017/S175907870999064X Published online by Cambridge University Press